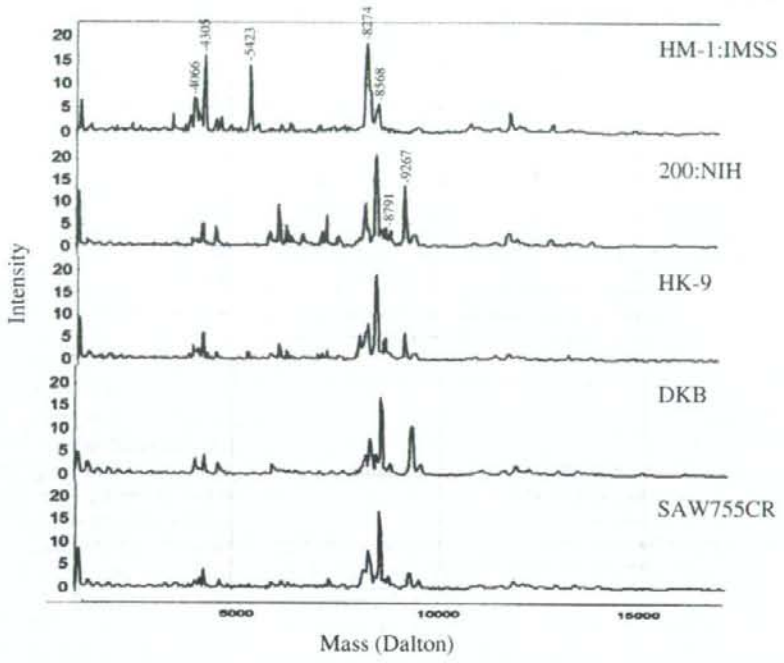

Fig. 2 Representative SELDI-TOF MS spectra of five laboratory strains of *E. histolytica*. The molecular masses are shown above the peaks

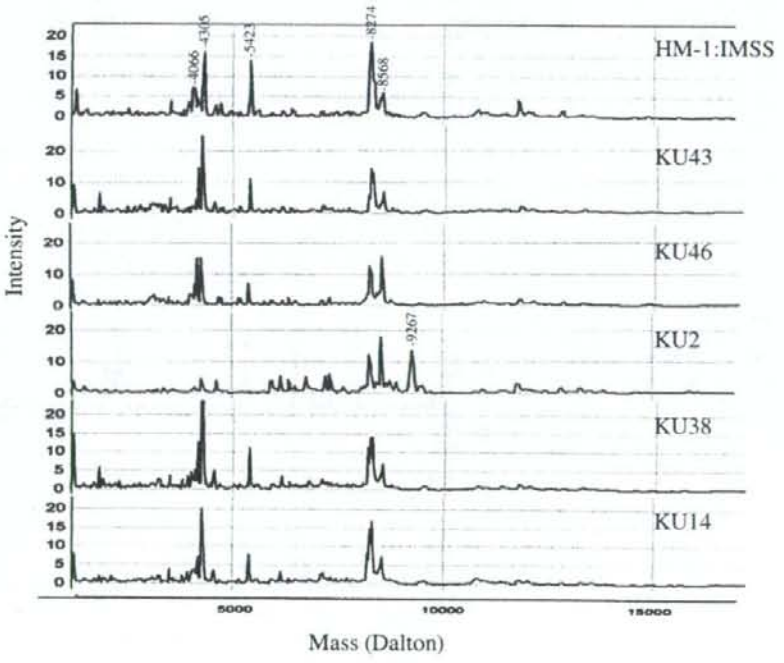

Fig. 3 Representative SELDI-TOF MS spectra of five Japanese isolates of *E. histolytica*. The molecular masses are shown above the major peaks

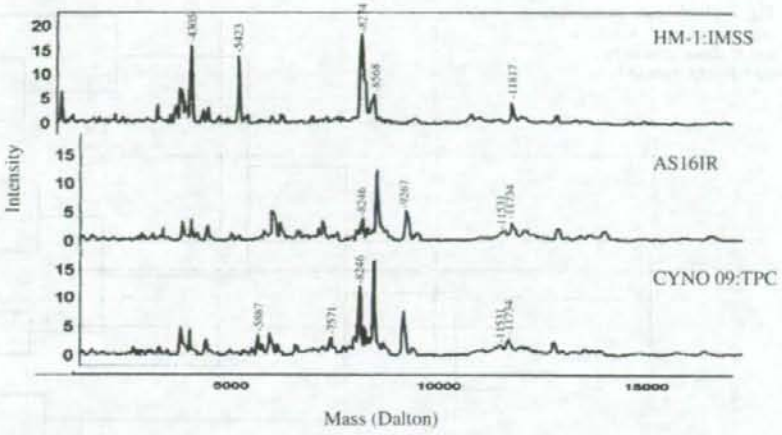

Fig. 4 Representative SELDI-TOF MS spectra of *E. dispar* isolates. The molecular masses are shown above the major peaks

peaks of 4.305 and 5.423 kDa were significantly lower than those of HM-1:IMSS, which was similar to the *E. histolytica* laboratory strains except HM-1:IMSS. The peak of 5.887 kDa was detected only in CYNO 09:TPC. The peaks of AS16IR and CYNO 09:TPC were mostly low in the range of 6–8 kDa, and the peak of 7.571 kDa was observed only in CYNO 09:TPC. In the range of 8–10 kDa, the major peak of 8.274 kDa common to *E. histolytica* isolates was not seen in either isolate of *E. dispar*, but the peak of 8.246 kDa was observed. Furthermore, like the *E. histolytica* laboratory strains except HM-1:IMSS, the peak of 8.568 kDa was significantly higher than that of HM-1:IMSS. The peak of 9.267 kDa, which was not seen in HM-1:IMSS, was observed in both isolates. In the range of 10–15 kDa, two peaks of 11.531 and 11.734 kDa not detected in *E. histolytica* were detected in both isolates of *E. dispar* (Fig. 4).

Similarity of peak patterns by SELDI-TOF MS among *E. histolytica* and *E. dispar* isolates and a dendrogram by the UPGMA method

The HM-1:IMSS showed 38.4 (200:NIH) to 69.2% (KU38 and KU14) similarity against other *E. histolytica* isolates, and KU38 and KU14 showed the highest similarity of 96.9% (Fig. 5). *E. dispar* AS16IR and CYNO 09:TPC showed 81.5% similarity to each other and were most associated with *E. histolytica* DKB, showing 72.3% similarity. The dendrogram representing relations among *E. histolytica* and

Fig. 5 Similarity of protein profiles among *E. histolytica* and *E. dispar* isolates. Percentage similarities were determined as described in Materials and methods

	HM-1:IMSS	200:NIH	HK-9	DKB	SAW755CR	KU43	KU46	KU2	KU38	KU14	AS16IR	CYNO09:TPC
HM-1:IMSS												
200:NIH	38.4											
HK-9	50.8	81.5										
DKB	53.8	76.9	81.5									
SAW755CR	44.6	70.8	83.1	87.7								
KU43	56.9	50.8	64.6	63.1	58.5							
KU46	49.2	56.9	70.8	70.8	63.1	67.7						
KU2	41.5	83.1	75.4	78.5	70.8	44.6	61.5					
KU38	69.2	55.4	72.3	70.8	67.7	84.6	83.1	60.0				
KU14	69.2	58.5	73.8	80.0	72.3	83.1	83.1	63.1	96.9			
AS16IR	38.5	61.5	61.5	72.3	61.5	47.7	44.6	55.4	58.5	56.9		
CYNO09:TPC	29.2	53.8	58.5	72.3	63.1	44.6	46.2	43.1	47.7	55.4	81.5	

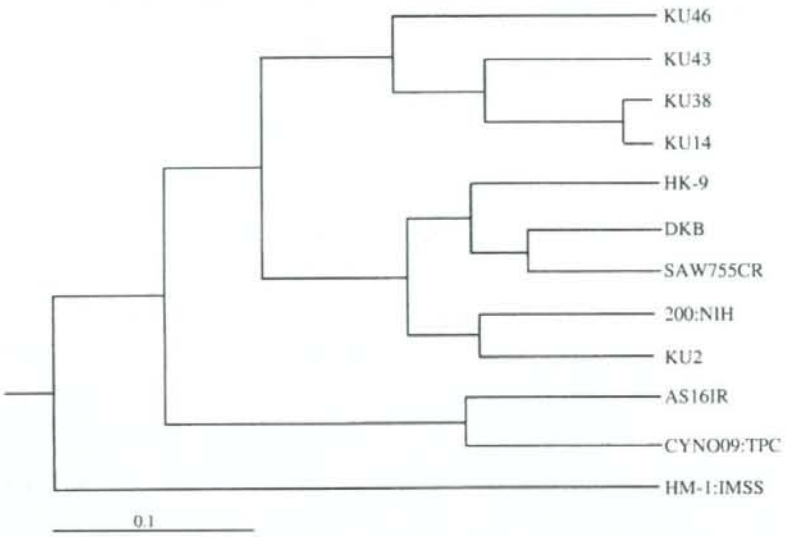

Fig. 6 Dendrogram representing relations among *E. histolytica* and *E. dispar* isolates by the UPGMA method

E. dispar isolates indicates that HM-1:IMSS is in an independent clade separated from other *E. histolytica* isolates, and two isolates of *E. dispar* were in one clade (Fig. 6). In two other clades, one includes KU46, KU43, KU38, and KU14, and the other includes HK-9, DKB, SAW755CR, 200:NIH, and KU2. DKB and SAW755CR, and 200:NIH and KU2, as well as KU38 and KU14 were included in the same clades, respectively (Fig. 6).

Discussion

ProteinChip technology is a new technology used to study proteomic profiles in biological samples, such as serum, cerebrospinal fluid, and cell or tissue extracts (Merchant and Weinberger 2000; Wulfkuhle et al. 2001; Carrette et al. 2003; Luo et al. 2003; Carlson et al. 2004) and is used in biomarker discovery and protein profiling (Ball et al. 2002; Choe et al. 2002; Yasui et al. 2003; Hayman and Przyborski 2004). With regard to parasitic protozoa, this technology was first used to detect antigens in sera of patients with African trypanosomiasis as a novel diagnostic method (Papadopoulos et al. 2004).

The heterogeneity of several DNA loci, including protein-coding sequences, has been extensively characterized among *E. histolytica* and *E. dispar* isolates (Clark and Diamond 1993; Ghosh et al. 2000; Zaki and Clark 2001; Zaki et al. 2002; Haghighi et al. 2002; Haghighi et al. 2003), and the overall genomic diversity among them has also been reported (Shah et al. 2005). However, there have been few reports on protein profiling among isolates of the two *Entamoeba* species. In this study, we used SELDI-TOF MS ProteinChip technology to identify protein patterns in different isolates of *E. histolytica* and showed phenotypic heterogeneity of proteins among them even under identical culture conditions. The results clearly indicate differences in SELDI-TOF MS spectra between the HM-1:IMSS and the other four laboratory strains and also between the HM-1:IMSS and the Japanese isolates, independent of their zymodemes. The HM-1:IMSS, which is most widely used as a standard strain, was in a separate clade in the dendrogram from the other *E. histolytica* isolates. Although the reason for this remains unclear, it should be taken into consideration when *E. histolytica* HM-1:IMSS as a standard strain is compared with other *Entamoeba* species. The percentage similarity in peak patterns among the isolates did not distinguish *E. dispar* from *E. histolytica*. It is clear from comparison of protein profiles between *E. histolytica* and *E. dispar* that there are peaks specific for each species of amoeba. These could be useful markers for distinguishing the two species, although the number of *E. dispar* isolates used in this study is limited.

Two-dimensional polyacrylamide gel electrophoresis (2D-PAGE) has been the most commonly used method for proteomic analysis (GÖrg et al. 2004), but the need for protein staining and the subsequent sample handling limits the sensitivity of the overall approach (Issaq et al. 2002). The 2D-PAGE is also laborious, difficult to automate, has poor resolution for extreme masses and extreme acidic or basic proteins, and requires large amount of starting material. The 2D-PAGE has recently been used for proteome of *E. histolytica* HM-1:IMSS trophozoites (Leitsch et al. 2005).

If 2D-PAGE is used for analysis of a number of different isolates of *E. histolytica* and *E. dispar*, it would be very laborious, time consuming, and difficult to analyze. In this respect, SELDI-TOF MS ProteinChip technique has an advantage over 2D-PAGE.

There is a wide variety of clinical manifestations observed among individuals infected with *E. histolytica* and/or *E. dispar*. What determines these differences remains unclear. In this respect, studies on phenotypic differences in proteins other than genetic heterogeneity are important and would contribute to resolving the question because the proteome, compared with the genome, provides a more realistic view of a biological status and is, therefore, expected to be more useful than gene analysis for evaluating disease presence and progression and response to treatment (Engwegen et al. 2006). Thus, proteomics can bridge the gap between the genome sequence and cellular behavior.

Finally, SELDI-TOF MS ProteinChip technique was successfully used to analyze different isolates of *E. histolytica* and *E. dispar*. Using the different array surfaces, a complete picture of each strain of *Entameoba* may be drawn, and thus a better set of protein fingerprint profiles for each strain would be provided. Like the successful application of this technology to bacterial proteomes (Barzaghi et al. 2004), the results show the usefulness of ProteinChip technology for studying the proteomics of parasitic protozoa as well, alone or in combination with other technologies.

Acknowledgments We thank N Watanabe for his valuable discussion with us, T Obata for SELDI-TOF MS ProteinChip analysis, and T Yamashita for her technical assistance. This work was supported by a Health Science Research Grant for Research on Emerging and Re-emerging Infectious Diseases from the Ministry of Health, Labor and Welfare of Japan.

References

Ball G, Mian S, Holding F, Allibone RO, Lowe J, Ali S, Li G, McCardle S, Ellis IO, Creaser C, Rees RC (2002) An integrated approach utilizing artificial neural networks and SELDI mass spectrometry for the classification of human tumours and rapid identification of potential biomakers. Bioinformatics 18:395–404

Barzaghi D, Isbister JD, Lauer KP, Born TL (2004) Use of surface-enhanced laser desorption/ionization-time of flight to explore bacterial proteomes. Proteomics 4:2624–2628

Carlson KA, Ciborowski P, Schellpeper CN, Biskup TM, Shen RF, Luo X, Destache CJ, Gendelman HE (2004) Proteomic fingerprinting of HIV-1-infected human monocyte-derived macrophages: a preliminary report. J Neuroimmunol 147:35–42

Carrette O, Demalte I, Scherl A, Yalkinoglu O, Corthals G, Burkhard P, Hochstrasser DF, Sanchez JC (2003) A panel of cerebrospinal fluid potential biomarkers for the diagnosis of Alzheimer's disease. Proteomics 3:1486–1494

Cheng X-J, Tachibana H, Kobayashi S, Kaneda Y, Huang M-Y (1993) Pathogenicity of *Entamoeba histolytica* isolates from Shanghai, China. Parasitol Res 79:608–610

Choe LH, Dutt MJ, Relkin N, Lee KH (2002) Studies of potential cerebrospinal fluid molecular markers for Alzheimer's disease. Electrophoresis 23:2247–2251

Clark CG, Diamond LS (1993) *Entamoeba histolytica*: a method for isolate identification. Exp Parasitol 77:450–455

Diamond LS, Harlow DR, Cunnick CC (1978) A new medium for the axenic cultivation of *Entamoeba histolytica* and other *Entamoeba*. Trans R Soc Trop Med Hyg 72:431–432

Engwegen JYMN, Gast MC, Schellens JHM, Beijnen JH (2006) Clinical proteomics: searching for better tumour markers with SELDI-TOF mass spectrometry. Trends Pharmacol Sci 27:251–259

Ghosh S, Frisardi M, Ramirez-Avila L, Descoteaux S, Sturm-Ramirez K, Newton-Sanchez OA, Santos-Preciado JI, Ganguly C, Lohia A, Reed S, Samuelson J (2000) Molecular epidemiology of *Entamoeba* spp.: evidence of a bottleneck (demographic sweep) and transcontinental spread of diploid parasites. J Clin Microbiol 38:3815–3821

Görg A, Weiss W, Dunn MJ (2004) Current two-dimensional electrophoresis technology for proteomics. Proteomics 4:3665–3685

Haghighi A, Kobayashi S, Takeuchi T, Masuda G, Nozaki T (2002) Remarkable genetic polymorphism among *Entamoeba histolytica* isolates from a limited geographic area. J Clin Microbiol 40:4081–4090

Haghighi A, Kobayashi S, Takeuchi T, Thammapalerd N, Nozaki T (2003) Geographic diversity among genotypes of *Entamoeba histolytica* field isolates from a limited geographic area. J Clin Microbiol 41:3748–3756

Hayman MW, Przyborski SA (2004) Proteomic identification of biomarkers expressed by human pluripotent stem cells. Biochem Biophys Res Commun 316:918–923

Hutchens TW, Yip TT (1993) New desorption strategies for the mass spectrometric analysis of macromolecules. Rapid Commun Mass Spectrom 7:576–580

Issaq HJ, Veenstra TD, Conrad TP, Felschow D (2002) The SELDI-TOF MS approach to proteomics: protein profiling and biomarker identification. Biochem Biophys Res Commun 292:587–592

Kobayashi S, Imai E, Haghighi A, Khalifa SA, Tachibana H, Takeuchi T (2005) Axenic cultivation of *Entamoeba dispar* in newly desighed yeast extract-iron–gluconic acid–dihydroxyacetone–serum medium. J Parasitol 91:1–4

Leitsch D, Radauer C, Paschinger K, Wilson IB, Breiteneder H, Scheiner O, Duchene M (2005) *Entamoeba histolytica*: analysis of the trophozoite proteome by two-dimensional polyacrylamide gel electrophoresis. Exp Parasitol 110:191–195

Luo X, Carlson KA, Wojna V, Mayo R, Biskup TM, Stoner J, Anderson J, Gendelman HE, Melendez LM (2003) Macrophage proteomic fingerprinting predicts HIV-1-associated cognitive impairment. Neurology 60:1931–1937

Merchant M, Weinberger SR (2000) Recent advancements in surface enhanced laser desorption/ionization-time of flight-mass spectrometry. Electrophoresis 21:1164–1177

Papadopoulos MC, Abel PM, Stich A, Tarelli E, Bell BA, Planche T, Loosemore A, Saadoun S, Wilkins P, Krishna S (2004) A novel and accurate diagnostic test for human African trypanosomiasis. Lancet 363:1358–1363

Sargeaunt PG (1988) Zymodemes of *Entamoeba histolytica*. In: Radvin JI (ed) Amebiasis: human infection by *Entamoeba histolytica*. Wiley, New York, pp 370–387

Shah PH, MacFarlane RC, Bhattacharya D, Matese JC, Demeter J, Stroup SE, Singh U (2005) Comparative genomic hybridizations of *Entamoeba* strains reveal unique genetic fingerprints that correlate with virulence. Eukaryotic Cell 4:504–515

Tachibana H, Kobayashi S, Takekoshi M, Ihara S (1991) Distinguishing pathogenic isolates of *Entamoeba histolytica* by polymerase chain reaction. J Infect Dis 164:825–826

WHO/PAHO/UNESCO (1997) A consultation with experts on amebiasis. Epidemiol Bull 18:13–14

Wulfkuhle JD, McLean KC, Paweletz CP, Sgroi DC, Trock BJ, Steeg PS, Petricoin EF III (2001) New approaches to proteomic analysis of breast cancer. Proteomics 1:1205–1215

Yasui Y, Pepe M, Thompson ML, Adam BL, Wright GL Jr, Qu Y, Potter JD, Winget M, Thornquist M, Feng Z (2003) A data-analytic strategy for protein biomarker discovery: profiling of high-dimensional proteomic data for cancer detection. Biostatistics 4:449–463

Zaki M, Clark CG (2001) Isolation and characterization of polymorphic DNA from *Entamoeba histolytica*. J Clin Microbiol 39:897–905

Zaki M, Meelu P, Sun W, Clark CG (2002) Simultaneous differentiation and typing of *Entamoeba histolytica* and *Entamoeba dispar*. J Clin Microbiol 40:1271–1276

Primary structure, expression and localization of two intermediate subunit lectins of *Entamoeba dispar* that contain multiple CXXC motifs

H. TACHIBANA[1]*, X.-J. CHENG[1], S. KOBAYASHI[2], Y. OKADA[3], J. ITOH[3] *and* T. TAKEUCHI[2]

[1] *Department of Infectious Diseases and* [2] *Teaching and Research Support Center, Tokai University School of Medicine, Isehara, Kanagawa 259-1193, Japan*
[3] *Department of Tropical Medicine and Parasitology, Keio University School of Medicine, Shinjuku-ku, Tokyo 160-8582, Japan*

(*Received 29 May 2007; revised 25 June 2007; accepted 4 July 2007; first published online 6 September 2007*)

SUMMARY

We have recently identified 2 surface proteins in *Entamoeba histolytica* as intermediate subunits of galactose- and *N*-acetyl-D-galactosamine-inhibitable lectin (EhIgl1 and EhIgl2); these proteins both contain multiple CXXC motifs. Here, we report the molecular characterization of the corresponding proteins in *Entamoeba dispar*, which is neither pathogenic nor invasive. Two *Igl* genes encoding 1110 and 1106 amino acids (EdIgl1 and EdIgl2) were cloned from 2 strains of *E. dispar*. The amino acid sequence identities were 79% between EdIgl1 and EdIgl2, 75–76% between EdIgl1 and EhIgl1, and 73–74% between EdIgl2 and EhIgl2. However, all the CXXC motifs were conserved in the EdIgl proteins, suggesting that the fold conferred by this motif is important for function. Comparison of the expression level of the *Igl* genes by real-time RT-PCR showed 3–5 times higher expression of *EdIgl1* compared to *EdIgl2*. Most EdIgl1 and EdIgl2 proteins were co-localized on the surface and in the cytoplasm of trophozoites, based on confocal microscopy. However, a different localization of EdIgl1 and EdIgl2 in intracellular vacuoles and a different level of phenotypic expression of the two Igls were also observed. These results demonstrate that Igls are important proteins even in non-pathogenic amoeba and that Igl1 and Igl2 may possess different functions.

Key words: *Entamoeba dispar*, *Entamoeba histolytica*, intermediate subunit of Gal/GalNAc lectin (Igl), cysteine-rich protein.

INTRODUCTION

It has been estimated that 480 million people worldwide are infected with *Entamoeba histolytica* or *Entamoeba dispar* (Walsh, 1986). *E. histolytica* is the causative agent of human amoebic colitis and liver abscess, which result in up to 110000 deaths annually. *E. dispar* is morphologically indistinguishable from *E. histolytica*, but is non-pathogenic and non-virulent (Diamond and Clark, 1993). Adherence of *E. histolytica* trophozoites to host cells is an essential step in its pathogenicity, and it is well known that the 170 kDa heavy subunit of galactose- and *N*-acetyl-D-galactosamine (Gal/GalNAc)-inhibitable lectin (Hgl) is the key factor in adherence and subsequent pathogenesis of the amoeba (Petri *et al.* 2002). Hgl is a transmembrane protein that forms a heterodimer with a glycosylphosphatidylinositol (GPI)-anchored 35 kDa light subunit (Lgl) via disulfide bonds (Petri *et al.* 1989). Recently, we have identified a GPI-anchored 150 kDa intermediate subunit (Igl) of lectin, which is non-covalently associated with Hgl (Cheng *et al.* 1998, 2001). There are 2 isoforms of Igl, which consist of 1101 and 1105 amino acids and are referred to as Igl1 and Igl2, respectively; both are cysteine-rich proteins containing multiple CXXC motifs. A mouse monoclonal antibody (mAb) to Igl significantly inhibits adherence and cytotoxicity of trophozoites to mammalian cells *in vitro* and also inhibits liver abscess formation in hamsters (Tachibana *et al.* 1997; Cheng *et al.* 1997, 1999). Antibodies to Igl have been detected not only in symptomatic patients with amoebiasis but also in asymptomatic cyst passers of *E. histolytica* (Tachibana *et al.* 2004). Immunization of hamsters with affinity-purified Igl can prevent amoebic liver abscess formation (Cheng and Tachibana, 2001), and Igl has also been detected in the *E. histolytica* fraction that interacts with the brush border of enterocytes (Seigneur *et al.* 2005). Therefore, Igl seems to be one of the key molecules in amoebic adherence to host cells and pathogenicity; however, the correlation of these effects with

* Corresponding author: Department of Infectious Diseases, Tokai University School of Medicine, Isehara, Kanagawa 259-1193, Japan. Tel: +81 463 93 1121. Fax: +81 463 95 5450. E-mail: htachiba@is.icc.u-tokai.ac.jp

Parasitology (2007), **134**, 1989–1999. © 2007 Cambridge University Press
doi:10.1017/S0031182007003459 Printed in the United Kingdom

each Igl isoform and the differences between the isoforms are not known.

Comparison of *E. histolytica* and *E. dispar* is also of importance for understanding the pathogenicity of amoeba. One well-known difference between the two species is associated with the family of cysteine proteases that are pathogenic factors in *E. histolytica*; in *E. dispar*, the *EhCP1* gene is absent and *EhCP5* is degenerate (Bruchhaus *et al.* 1996; Willhoeft *et al.* 1999). Concerning lectins, it has been reported that Hgl is present in *E. dispar*, but that its expression level is lower than that in *E. histolytica* (Pillai *et al.* 1997, 2001). Therefore, it is of interest to determine if Igl1 and Igl2 are expressed in *E. dispar*. We report here the primary structure of the 2 Igl isoforms in 2 *E. dispar* strains isolated from human and cynomolgus monkey, respectively. We also compared the expression levels of *Igl* genes between *E. dispar* and *E. histolytica*, and examined the expression and localization of Igl1 and Igl2 in *E. dispar*.

MATERIALS AND METHODS

Cultivation of parasites

Trophozoites of the *E. dispar* SAW1734RclAR strain were grown axenically or monoxenically with sterilized *Crithidia fasciculata* in YIGADHA-S medium supplemented with 15% adult bovine serum at 37 °C (Kobayashi *et al.* 2005; Khalifa *et al.* 2006). Trophozoites of the *E. dispar* CYNO9:TPC strain were axenically cultured in the YIGADHA-S medium. Trophozoites of *E. histolytica* HM-1:IMSS were axenically cultured in TYI-S-33 medium supplemented with 15% adult bovine serum at 37 °C (Diamond *et al.* 1978). Cultured trophozoites were harvested in the logarithmic phase of growth and used in subsequent experiments.

Construction of a cDNA library and cloning of the Igl *gene*

Poly(A) RNA of *E. dispar* SAW1734RclAR trophozoites was isolated using a QuickPrep mRNA purification kit (Amersham Pharmacia). A cDNA library was constructed from 5 μg of poly(A) RNA using a cDNA synthesis kit (Amersham Pharmacia) and a λgt11 vector kit (Stratagene). The library was screened with a 657 bp probe using the Gene Images AlkPhos Direct labelling and detection system (Amersham Pharmacia). The probe was prepared from plasmid DNA containing the *E. histolytica Igl1* gene by PCR amplification using primers EhIgl1-S877 (5′-CCC TCG AGT CAA ATG GTG AAT GTA AGC C-3′) and Ehlgl1-AS1088 (5′-CCC TCG AGT TAA ATG CCT TTA GCT CCA TT-3′) (Tachibana *et al.* 2004). The positive clone containing the longest insert was subcloned into a pUC19 vector and sequenced. To extend the sequence of the 5′ end, rapid amplification of the cDNA end was performed with a 5′-Full RACE Core Set (Takara). For the cloning of the other *Igl* gene, the cDNA library was subjected to PCR using primers 5′-CAA TTT CAC TTG GTG AGT ACA AAG CTG-3′ (forward) and 5′-GAA AAT TCC TTT ACT TCC ATT GCA GTT TCC-3′ (reverse). These primers were prepared based on the sequence of the first cloned *E. dispar Igl* gene, with reference to the location of common sequences between the two *E. histolytica Igl* genes. The amplified genes were cloned using a TOPO TA Cloning Kit (Invitrogen) and sequenced. To extend the sequence of the 5′ and 3′ ends of the cloned DNA, a 5′-Full RACE Core Set and 3′-Full RACE Core Set were used (Takara). For the cloning of *Igl* genes from the CYNO9:TPC strain, genomic DNA isolated as previously described (Tachibana *et al.* 1991) was used as a template for PCR, using the forward primers 5′-ATG TTT ATT ATT CTT TTA TTC ATA TCA ATT TCA C-3′ (*Igl1*) and 5′-ATG TTT ATT CTT CTT TTA TTT ATA TCA ATT TCA C-3′ (*Igl2*), and the reverse primer 5′-TTA GAA CAT AAA TGA TAA CAT GAC TAT CAC CAT C-3′. Thirty-five cycles of PCR using *Pyrobest* DNA polymerase (Takara) were performed as follows: denaturation at 94 °C for 15 s (195 s in cycle 1), annealing at 58 °C for 30 s, and polymerization at 72 °C for 180 s (600 s in cycle 35). Amplified DNA was cloned using a Zero Blunt TOPO PCR Cloning Kit (Invitrogen) and sequenced. Nucleotide sequence data were analysed using Genetyx-Mac ver. 11.

Southern blot analysis

Genomic DNA was isolated from *E. dispar* SAW-1734RclAR trophozoites as described previously (Tachibana *et al.* 1991). Three μg of genomic DNA was digested with restriction enzymes *Dra*I, *Taq*I and *Hin*dIII. The fragments were separated on a 1% agarose gel, transferred to a Hybond N^+ membrane (Amersham Pharmacia) by capillary action, and fixed by alkaline denaturation. The membrane was hybridized at 55 °C in buffer containing a Gene Images AlkPhos Direct-labelled probe (Amersham Pharmacia) prepared by PCR amplification of cloned cDNA. The primers used for amplification were 5′-AGA TGG ATT CTA TTT TGA TGA-3′ (forward) and 5′-CAT ATG TCT TGA ACA TGG-3′ (reverse). The blots were detected using a CDP-star detection reagent (Amersham Pharmacia) and exposed to autoradiography films.

Real-time RT-PCR analysis

Total RNAs of *E. dispar* and *E. histolytica* trophozoites isolated using an RNeasy mini kit (Qiagen) were used for cDNA synthesis with a GeneAmp RNA PCR kit (Applied Biosystems). Reaction mixtures for quantitative real-time PCR analysis were

prepared using SYBR Premix Ex *Taq* (Takara), specific primers, Rox dye, and the cDNAs. The primers used were as follows: 5′-TGA CAA AGA CAA TAC TTG TAA AAA GTG-3′ (forward) and 5′-ATT ACT AAC ACA TGC ACA TTT TTT GTC-3′ (reverse) for *E. dispar Igl1* genes; 5′-TCG ATG AAA ATA ATG TAT GCC AGA AAT-3′ (forward) and 5′-TCA TCA AGG CAA GCA CAT TGA CTG-3′ (reverse) for *E. dispar Igl2* genes; 5′-GTT CAC AGG TTG GTG CTT GTA CG-3′ (forward) and 5′-ACA GTA CAT GGC TTT TCT CCG GTA-3′ (reverse) for *E. histolytica Igl1* genes; 5′-GAT TCA CAA ACA AAG GAG TGT GCC-3′ (forward) and 5′-GTG CAT TTG AAC CAC TAG CAG CAA-3′ (reverse) for *E. histolytica Igl2* genes; and 5′-CCA GCT ATG TAT GTT GGA ATT CAA G-3′ (forward) and 5′-GAT CAA GTC TAA GAA TAG CAT GTG G-3′ (reverse) for *actin* genes. Forty cycles of amplification with recording of fluorescence intensity in each cycle were performed using an ABI PRISM 7700 Sequence Detection System (Applied Biosystems). After initial denaturation at 95 °C for 10 sec, a shuttle PCR protocol consisting of denaturation at 95 °C for 5 sec and annealing-extension at 60 °C for 30 sec was applied. Relative quantitation with data from the ABI PRISM 7700 Sequence Detection System software version 1.7 was performed by the comparative C_T method, using the actin gene as an internal standard. The experiments were repeated 3 times, including the steps of culture of trophozoites and isolation of RNA.

Expression of recombinant Igl1 *and* Igl2

DNA fragments encoding full-length Igls, except for the N-terminus and C-terminus signal sequences, were obtained by PCR amplification of cloned *Igl* genes. Primers EdIgl1-S14-Xho (5′-CCC TCG AGG AGT ACA AAG CTG ATA AAC T-3′) and EdIgl-AS-Xho (5′-CCC TCG AGT TAA ATT CCT TTA CTT CCA TT-3′) were used for amplification of the *Igl1* gene of SAW1734RclAR. For amplification of the *Igl2* gene of SAW1734RclAR, primers EdIgl2-S14-Xho (5′-CCC TCG AGG ATT ACA AAG CTG ATA AAC TCA TC-3′) and EdIgl-AS-Xho were used. PCR was performed as previously described (Tachibana *et al.* 2004). Each amplified DNA fragment was digested with *Xho*I, purified, and ligated with pET19b vector (Novagen). The plasmid was introduced into competent *Escherichia coli* JM109 cells and the direction and sequence of inserts were confirmed. *E. coli* BL21Star(DE3)pLysS cells (Invitrogen) were transformed with the cloned plasmids. Each clone was cultured in 400 ml of Luria-Bertani medium containing ampicillin until the culture reached an optical density of 0·6 at 600 nm. Isopropyl-*β*-D-thiogalactopyranoside was added to the cultures at a final concentration of 1 mM, and the cultures were incubated at 37 °C for 3 h. Preparation of inclusion bodies and refolding of the proteins were performed as previously described (Tachibana *et al.* 2004).

Production of specific mAbs

MAbs to Igl1 and Igl2 of *E. dispar* SAW1734RclAR were prepared as follows. Six-week-old male BALB/c mice were inoculated intraperitoneally with 10 μg of recombinant proteins in Freund's complete adjuvant and were inoculated again after 2 weeks. After an additional 3 weeks, the mice received only recombinant proteins. Four days later, spleen cells of immunized mice were isolated and fused with X63 Ag8.653 mouse myeloma cells using 50% polyethylene glycol 1500. Hybridomas secreting mAbs against *E. dispar* Igls were screened by immunofluorescent staining and ELISA, and were cloned by limiting dilution. Immunoglobulin isotypes of mAbs were determined by immunofluorescent staining using subtype-specific antibodies. Ascites was obtained by intraperitoneal inoculation of hybridomas into pristine-primed mice, and immunoglobulin was purified using an Affi-Gel protein A MAPS II kit (Bio-Lab).

Dot blot analysis

Recombinant Igls and sonicated trophozoites of *E. dispar* SAW1734RclAR were blotted on the nitrocellulose membrane using a Bio-Dot microfiltration apparatus (Bio-Rad). Filter strips were blocked with 3% bovine serum albumin (BSA) in phosphate-buffered saline (PBS) and reacted with mouse anti-*E. dispar* Igl mAbs for 30 min. After being washed with PBS containing 0·05% Tween-20 (PBS-Tween), the strips were incubated with horseradish peroxidase (HRP)-labelled goat anti-mouse IgG antibody (MP Biomedicals) for 30 min. The strips were then washed with PBS-Tween and developed with a Konica Immunostaining HRP-1000 kit.

SDS-PAGE and Western blot analysis

Recombinant Igl proteins or *E. dispar* trophozoites were treated with Laemmli's sample buffer (Laemmli, 1970) containing 2 mM phenylmethylsulfonyl fluoride, 2 mM *N*-*α*-*p*-tosyl-L-lysine chloromethylketone, 2 mM *p*-hydroxymercuriphenylsulfonic acid, and 4 μM leupeptin for 5 min at 95 °C and then subjected to sodium dodecyl sulfate-polyacrylamide gel electrophoresis (SDS-PAGE). Western blot analysis was performed as previously described (Tachibana *et al.* 2004).

Flow cytometry

Immunophenotypic surface staining of Igl1 and Igl2 using flow cytometry was performed on trophozoites of *E. dispar* SAW1734RclAR strain. Intact cells were incubated on ice with 3% BSA in PBS for 15 min, and then with a mixture of mAbs ED1-13 and ED2-1 for 15 min. After washing with ice-cold PBS, the cells were incubated with a mixture of Alexa Fluor 488-labelled goat anti-mouse IgG2b-specific antibody (Molecular Probes) and PE-labelled goat anti-mouse IgG1-specific antibody (Santa Cruz Biotechnology) for 15 min on ice. The cells were washed with ice-cold PBS and then fixed in 4% paraformaldehyde. Aliquots of approximately 5000 cells per sample were analysed using FACS Calibur (Becton Dickinson), with data analysis using CellQuest Software (BD Immunocytometry systems).

Confocal microscopy

E. dispar SAW1734RclAR trophozoites were fixed with 4% paraformaldehyde in PBS and attached to silane-coated glass slides using Shandon Cytospin 2. After washing with PBS, the glass slides were incubated with 10% sucrose in PBS for 1 h and then stored at −80 °C until use. For double staining of Igl1 and Igl2, fixed trophozoites on the slides were treated with 0·1% Triton X-100 in PBS for 5 min, blocked with 3% BSA in PBS for 30 min and then incubated for 1 h at room temperature with a mixture of 2 mAbs, ED1-13 and ED2-1. After washing, the slides were incubated with a mixture of Alexa Fluor 488-labelled goat anti-mouse IgG2b-specific antibody and Alexa Fluor 594-labelled goat anti-mouse IgG1-specific antibody (Molecular Probes) for 1 h. The stained trophozoites were mounted using glycerol containing 1·25 mg/ml 1,4-diazbicyclo(2,2,2)octane and 10% PBS, and the samples were observed using a Zeiss LSM510 META confocal laser scanning microscope.

RESULTS

Cloning of genes encoding E. dispar *Igl1 and Igl2*

Two *Igl* genes cloned from the cDNA library from the *E. dispar* SAW1734RclAR strain encoded proteins of 1110 and 1106 amino acids, respectively, with calculated molecular masses of 120·9 kDa and 120·3 kDa and theoretical p*I* values of 5·5 and 4·87, respectively (DDBJ, EMBL, and GenBank Accession numbers AB287423 and AB287424). Two *Igl* genes were also cloned from the genomic DNA of the *E. dispar* CYNO9:TPC strain. These genes also encoded proteins of 1110 and 1106 amino acids, respectively, with calculated molecular masses of 121·0 kDa and 120·4 kDa and theoretical p*I* values of 5·41 and 4·74, respectively (DDBJ, EMBL, and GenBank Accession numbers AB287425 and AB287426). Based on the similarity of the p*I* values to those of Igls of *E. histolytica* (5·52 for Igl1 and 5·17 for Igl2) (Cheng *et al.* 2001), the former protein was designated as Igl1 and the latter as Igl2 in both *E. dispar* strains. Multiple alignments of amino acid sequences among these Igl proteins and other *E. histolytica* Igls are shown in Fig. 1; the amino acid identity between *E. dispar* Igl1 and Igl2 was 79% in both strains. Differences in amino acids between the proteins in the two *E. dispar* strains were greater for Igl2 than for Igl1. In comparison with the *E. histolytica* Igl isoforms, the amino acid sequence identities were 75–76% for Igl1 and 73–74% for Igl2. Insertions of 6 amino acids in Igl1 and Igl2 are present in the two *E. dispar* strains around position 840. However, all cysteine residues found in *E. histolytica* Igl proteins were conserved in the *E. dispar* proteins. Both *E. dispar* Igl isoforms also contained hydrophobic amino- and carboxy-terminal signal sequences consistent with a GPI-anchored plasma membrane protein, and all Igl sequences contained a signature epidermal growth factor-like domain close to the C-terminus. The nucleotide sequence identities were 88% between the *E. dispar Igl1* and *Igl2* genes, 83% between the *E. dispar and E. histolytica Igl1* genes, and 82% between the *E. dispar* and *E. histolytica Igl2* genes.

A BLAST search of *E. dispar* SAW760 strain genomic sequences <http://www.ncbi.nlm.nih.gov/BLAST/>was performed, although the *E. dispar* genome project is incomplete. An identical sequence to that of the *Igl1* gene of the SAW1734-RclAR strain was found (Genbank Accession no. AANV01000026), and 2 sequences (AANV01000644 and AANV01001389) were identified that showed 99% identity with the *Igl2* gene of SAW1734RclAR in partially overlapping regions.

Southern blot analyses of Igl *genes*

Southern blot hybridization using a 420-bp PCR product as a probe was performed on *E. dispar* SAW1734RclAR genomic DNA digested with *Dra*I, *Taq*I and *Hin*dIII (Fig. 2). The results indicated the presence of 2 *Igl* genes in the *E. dispar* genomic DNA.

Real-time RT-PCR analysis of Igl *genes*

Expression levels of *Igl1* and *Igl2* are compared in Fig. 3. In the SAW1734RclAR strain, expression of *Igl1* was 3 times higher than that of *Igl2* ($P<0·001$), and in the CYNO9:TPC strain, expression of *Igl1* was 5 times higher than that of *Igl2* ($P<0·01$). Higher expression of *Igl1* compared to *Igl2* was also observed in *E. histolytica* ($P<0·001$). Expression of *Igl1* was lower in *E. dispar* than in *E. histolytica* (SAW1734RclAR *vs* HM-1:IMSS, $P<0·01$;

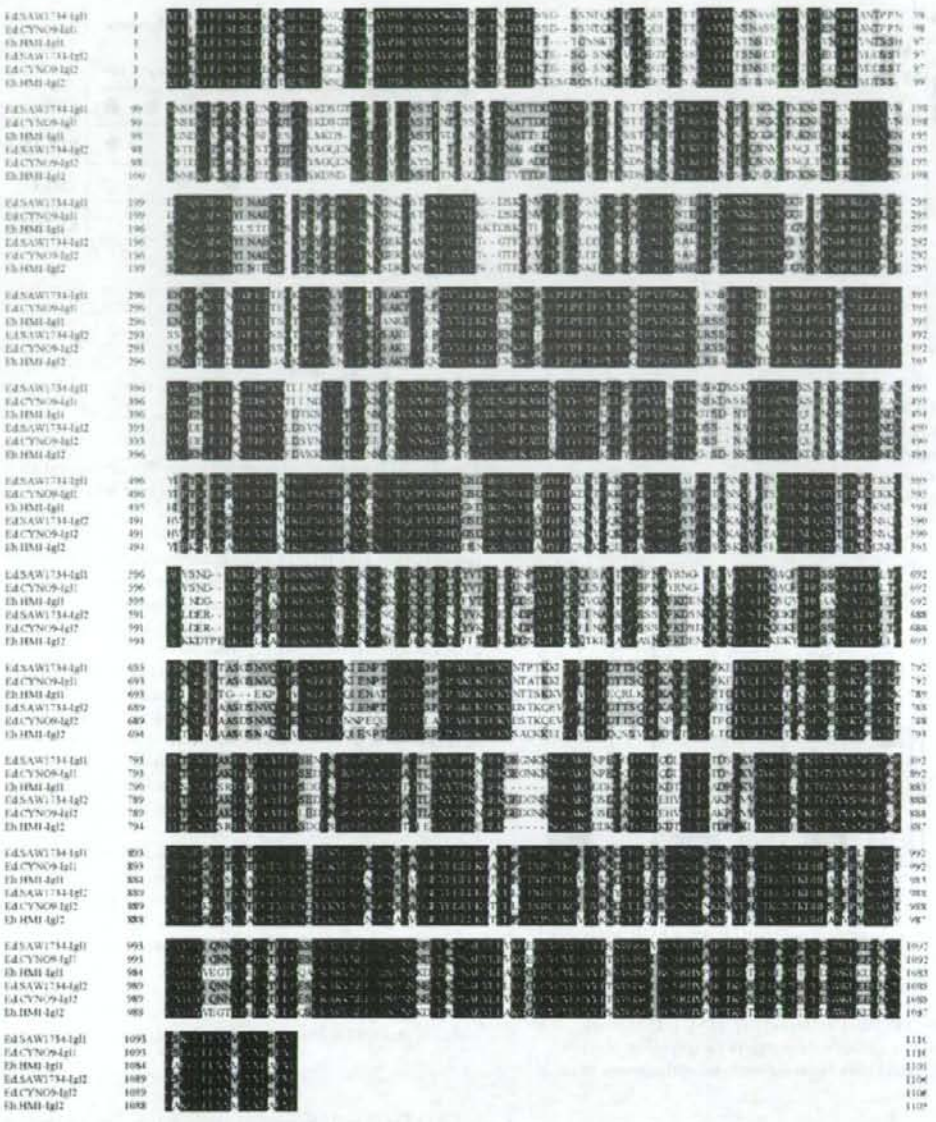

Fig. 1. Alignment of the deduced amino-acid sequences of the *Igl1* and *Igl2* genes from *Entamoeba dispar* SAW1734RclAR (Ed.SAW1734), *E. dispar* CYNO9:TPC (Ed.CYNO9) and *E. histolytica* HM-1:IMSS (Eh.HM1). Identical and conserved amino-acid residues are highlighted in black and grey, respectively.

CYNO9:TPC *vs* HM-1:IMSS, not significant), whereas *Igl2* expression was similar in the two species.

Dot blot and Western blot analyses of Igls

Full length (except for the signal sequence) recombinant *E. dispar* Igls from the SAW1724RclAR strain were prepared in *Escherichia coli*. The apparent molecular weight of the recombinant protein with the leader peptide was slightly larger for Igl2 (190 kDa) than for Igl1 (170 kDa) in SDS-PAGE under reducing conditions (data not shown). Recombinant Igl1 and Igl2 proteins were used for immunization of mice to prepare mAbs specific for each Igl. In dot blot analysis, mAb ED1-13 reacted specifically with recombinant Igl1, but not with recombinant Igl2; in contrast, mAb ED2-1 was

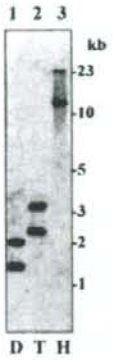

Fig. 2. Southern blot analysis of *Igl* genes in *Entamoeba dispar* SAW1734RclAR. Genomic DNA was digested with *Dra*I (D, lane 1), *Taq*I (T, lane 2) and *Hin*dIII (H, lane 3) and hybridized with the probe. The blot is representative of 2 independent experiments. Numbers to the right indicate the sizes of DNA markers (in kilobases).

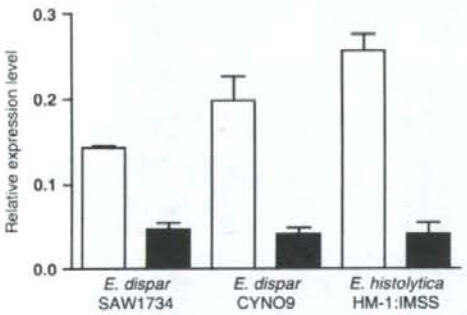

Fig. 3. Real-time reverse transcription PCR analysis of *Igl* genes from *Entamoeba dispar* and *E. histolytica*. Expression levels of *Igl1* (open bars) and *Igl2* (filled bars) in trophozoites from *E. dispar* SAW1734RclAR, *E. dispar* CYNO9:TPC and *E. histolytica* HM-1:IMSS are expressed as values relative to the expression level of *actin*. Vertical bars indicate the S.E. of the mean from 3 experiments.

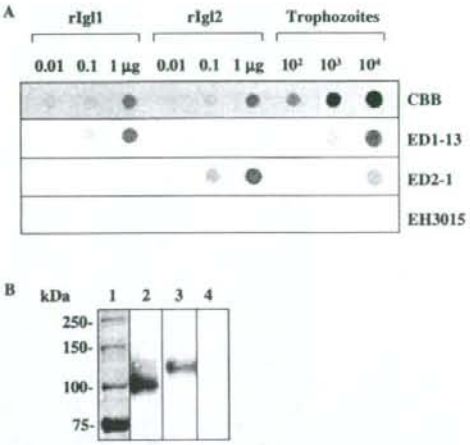

Fig. 4. (A) Reactivity of anti-Igl monoclonal antibodies to recombinant Igls and crude antigens of *Entamoeba dispar* in dot blot analysis. Various concentrations (0·01, 0·1 and 1 μg) of recombinant Igl1 (rIgl1) and recombinant Igl2 (rIgl2) and various numbers (10^2, 10^3 and 10^4) of sonicated trophozoites from strain SAW1734RclAR were spotted on nitrocellulose membranes. One strip was stained with Coomassie brilliant blue (CBB). Other strips were treated with anti-*E. dispar* Igl monoclonal antibodies (ED1-13, ED2-1) and anti-*E. histolytica* Igl monoclonal antibody (EH3015). HRP-conjugated goat antibody to mouse IgG was used as a secondary antibody. The blot is representative of 2 independent experiments. (B) Western immunoblot analysis of native Igls of *E. dispar*. Lysates of SAW1734RclAR trophozoites were subjected to SDS-PAGE in a 7·5% gel under non-reducing conditions and transferred to polyvinylidene difluoride membranes. Protein bands of the size marker in lane 1 were stained with Coomassie brilliant blue. The strips were treated with monoclonal antibodies as follows: lane 2, ED1-13; lane 3, ED2-1; and lane 4, EH3015. HRP-conjugated goat antibody to mouse IgG was used as a secondary antibody. The blot is representative of 3 independent experiments. The numbers to the left indicate molecular masses (in kilodaltons).

reactive specifically with recombinant Igl2 (Fig. 4A). In conditions under which the reactivity of these mAbs to *E. dispar* trophozoites was comparable, differences in reactivity to equal amounts of recombinant Igls were observed. The reactivity of mAb ED1-13 to 10^4 trophozoites was similar to the reactivity to 1 μg of EdIgl1, whereas the reactivity of mAb ED2-1 to 10^4 trophozoites were comparable to the reactivity to 0·1 μg of EdIgl2, suggesting that the amount of Igl2 was approximately one-tenth that of Igl1 in the trophozoites. In Western blot analysis using trophozoites from the SAW1734RclAR strain, mAbs ED1-13 and ED2-1 recognized a 100 kDa and a 120 kDa band, respectively, under non-reducing conditions (Fig. 4B). No bands were detected in the Western blot under reducing conditions, indicating that the mAbs recognized discontinuous epitopes on the Igl proteins.

Phenotypic expression of Igls on the surface of trophozoites

To compare the amounts of Igl1 and Igl2 expressed on the surface of trophozoites from the *E. dispar* SAW1724RclAR strain, flow cytometric analysis was performed using specific mAbs for each Igls (Fig. 5). The results demonstrated that almost all

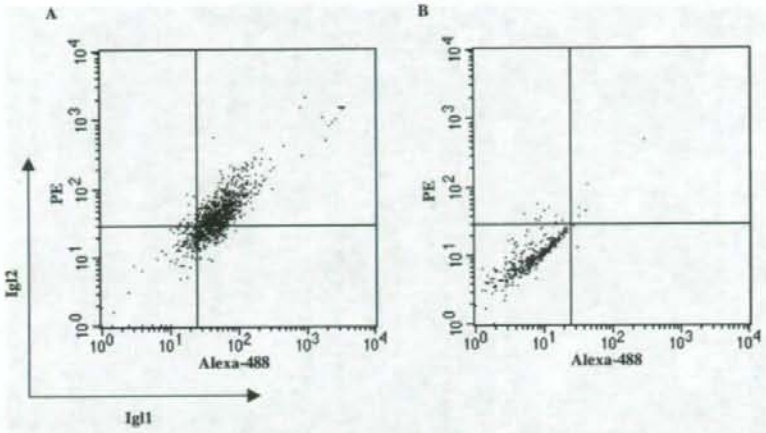

Fig. 5. Flow cytometric analysis of phenotypic expression of Igl1 and Igl2 on the surface of *Entamoeba dispar* trophozoites. Intact trophozoites from the SAW1734RclAR strain were double stained with monoclonal antibodies ED1-13 (specific for Igl1, IgG2b) and ED2-1 (specific for Igl2, IgG1), followed by Alexa Fluor 488-labelled goat anti-mouse IgG2b-specific antibody and PE-labelled goat anti-mouse IgG1-specific antibody (A). The control was stained only with secondary antibodies (B). The results are representative of 3 independent experiments.

trophozoites expressed both Igl1 and Igl2 on the cell surface.

Localization of Igls on trophozoites

Localization of Igl1 and Igl2 on *E. dispar* trophozoites was examined by confocal laser scanning microscopy using specific mAbs. Both Igls were localized on the plasma membrane and in cytoplasm in all trophozoites (Figs 6 and 7). However, the amount of each Igl in the trophozoites was variable, especially in the cytoplasm; that is, Igl1- and Igl2-dominant cells were present (arrows and arrowheads in Fig. 6). In addition, Igl1- and Igl2-dominant vacuoles were also observed within a single trophozoite (arrow and arrowhead in Fig. 7).

DISCUSSION

Comparison of the 2 *Igl* genes cloned from *E. dispar* with those from *E. histolytica* indicated differences in the sequences of the corresponding proteins in *E. dispar* and *E. histolytica* and in the 2 strains of *E. dispar*. However, all the cysteine residues, including the CXXC motifs, were conserved between species and between strains, which suggests that the fold of the protein is maintained and is important for its function. Amino acid identities of Igl1 and Igl2 within species (79% in *E. dispar* and 81% in *E. histolytica*; Cheng *et al.* 2001) were higher than those for each Igl between the 2 species (75–76% for Igl1 and 73–74% for Igl2). Insertions of 6 amino acids around position 840 in *E. dispar* were present in both Igl1 and Igl2, as shown in Fig. 1. Nucleotide identities of the 2 *Igl* genes were also higher within species, compared to the respective identities of the *Igl* genes between *E. dispar* and *E. histolytica*. These results suggest that duplication of the genes may have occurred after divergence of the species.

The properties of the Gal/GalNAc lectin of *E. histolytica* were demonstrated in a 150 kDa fraction purified by affinity chromatography using the *E. histolytica*-specific mAb EH3015 (Cheng *et al.* 1998). In addition, Igl1 and Igl2 of *E. histolytica* have been detected, in addition to Hgl and Lgl, in the protein fraction that binds specifically to GalNAc-BSA-coated magnetic beads (McCoy and Mann, 2005). However, when we performed a preliminary examination of the reactivity of recombinant Igls from *E. histolytica* and *E. dispar* with $GalNAc_{27}$-BSA by dot blot analysis and surface plasmon resonance, we could not prove that the recombinant proteins had sugar-binding properties (data not shown). Therefore, the Igls may exist as part of the lectin complex, perhaps with non-covalent association to another protein containing a sugar-binding site, with this association occurring either directly or being mediated by a third protein. Recently, it has been reported that Igl of *E. histolytica* is found in the protein fraction that interacts with purified brush border from human enterocytes (Seigneur *et al.* 2005). It has also been demonstrated that the 140 kDa fibronectin-binding molecule of *E. histolytica* (Talamas-Rohana *et al.* 1992) is identical with Igl2 (Hernandez-Ramirez *et al.* 2007). These observations indicate that Igls are important proteins for amoebic adherence to host cells, and since Igls are also expressed in the non-pathogenic amoeba, it seems likely that these proteins are important for colonization of amoebae in the large intestine.

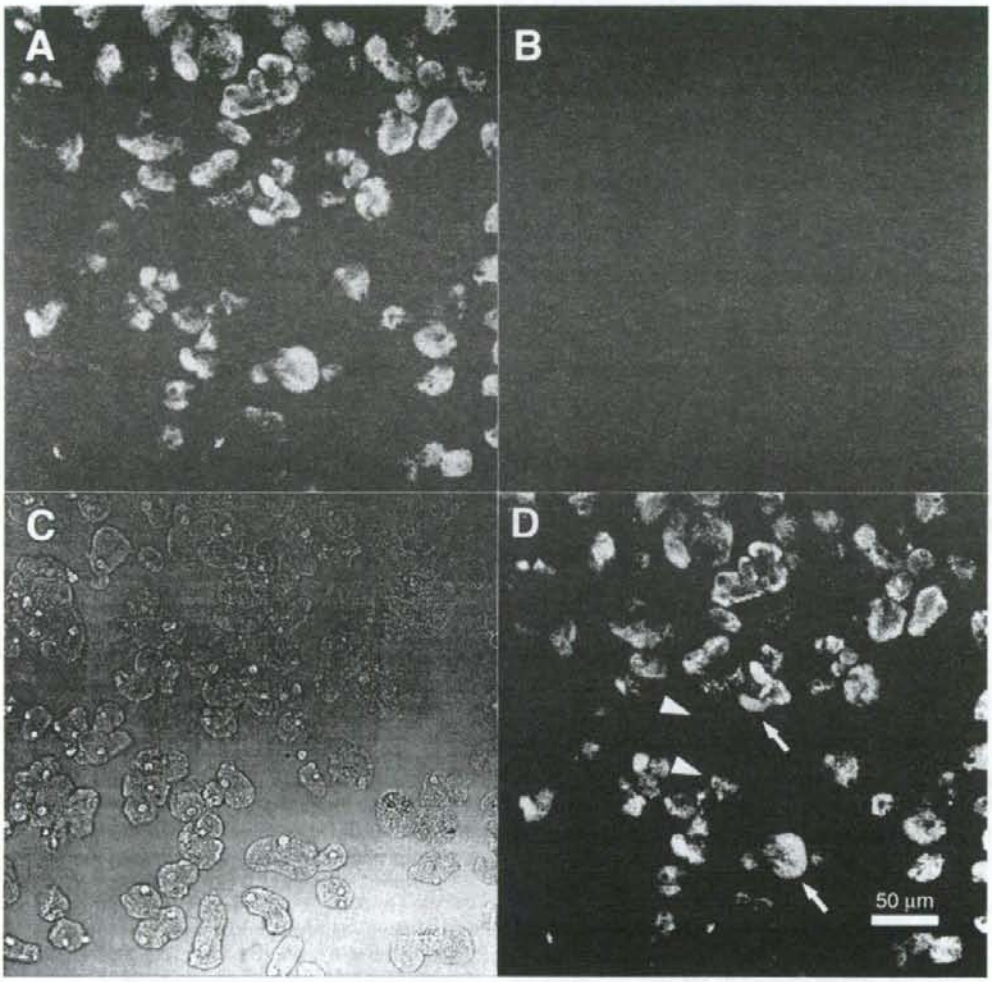

Fig. 6. Localization of Igl1 and Igl2 on trophozoites of *Entamoeba dispar* SAW1734RclAR observed by confocal laser scanning microscopy. Fixed trophozoites were stained with ED1-13 specific for Igl1 and a secondary Alexa Fluor 488-labelled anti-mouse IgG2b antibody (green) (A) or ED2-1 specific for Igl2 and a secondary Alexa Fluor 594-labelled anti-mouse IgG1 antibody (red) (B). Differential interference contrast microscopy is shown in (C). A merged image is shown in (D). Arrows and arrowheads indicate Igl1- and Igl2-dominant cells, respectively.

One of the interesting observations in this study is the difference in expression between Igl1 and Igl2. Since higher expression of Igl1 was observed at both protein and mRNA levels, the difference between the isoforms seems to be regulated mostly at the transcriptional level. The expression level of *Igl1* was also lower in *E. dispar* than in *E. histolytica*, whereas that of *Igl2* was comparable in the two species. It has been demonstrated that expression of *Hgl* (*Hgl2*) and *Lgl* (*Lgl1*) in *E. dispar* is lower than in *E. histolytica* (Pillai *et al.* 1997, 2001); therefore, Igl1 may be more closely associated with Hgl and Lgl. However, it is unknown whether the 2 Igl isoforms are associated with different isoforms of Hgl or Lgl. DNA microarray analyses have shown that a large number of genes are expressed differently in *E. histolytica* and *E. dispar*, and that there is a difference in gene expression between strains of *E. histolytica* of high and low virulence (Shah *et al.* 2005; MacFarlane and Singh, 2006; Davis *et al.* 2007). Lower expression of *Hgl* genes in *E. dispar* compared to *E. histolytica* has also been confirmed (MacFarlane and Singh, 2006), but *Lgl3* expression was found to be higher in an *E. histolytica* strain of low virulence compared to a strain of high virulence (Davis *et al.* 2007). *Igl* genes are down-regulated by

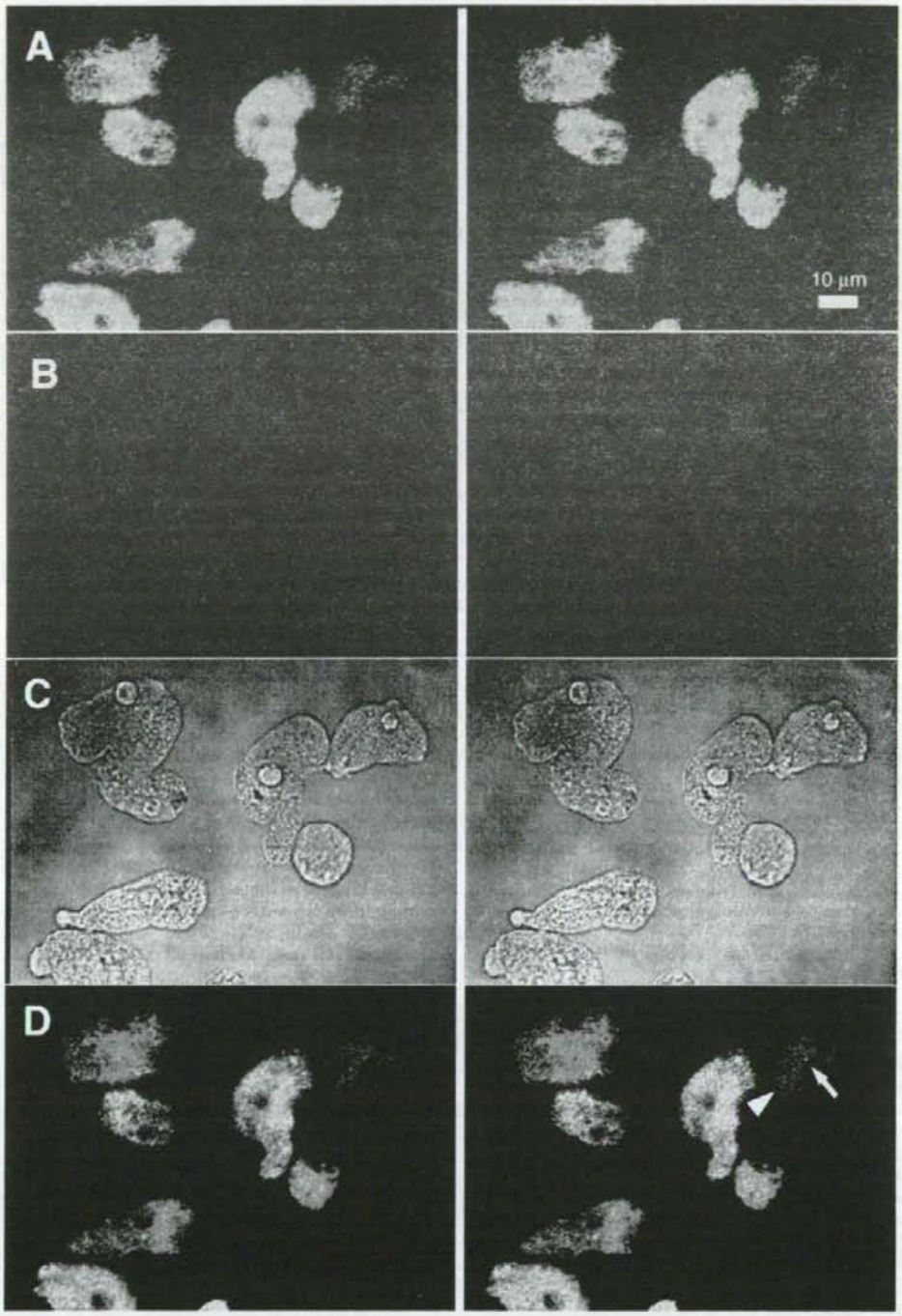

Fig. 7. Stereo images of localization of Igl1 (A) and Igl2 (B) on *Entamoeba dispar* trophozoites observed by confocal laser scanning microscopy. Fixed trophozoites were stained as described in Fig. 6. Differential interference contrast microscopy is shown in (C). A merged image is shown in (D). Arrow and arrowhead indicate single localization of Igl1 and Igl2, respectively.

heat shock stress, as are most *Hgl* and *Lgl* genes (Weber *et al.* 2006). Collectively, these observations suggest that the lectin as a whole is important for adherence and subsequent pathogenesis.

We also compared phenotypic expression of the two Igls in each trophozoite using flow cytometry and confocal microscopy. Interestingly, some trophozoites expressed Igl1 or Igl2 dominantly, although most cells expressed the two Igl proteins to a comparable extent, suggesting that both Igls are important for the amoeba. Igls were also localized in intracellular vacuoles of *E. dispar*. Recently, it has been demonstrated that Igl is contained in phagosomes of *E. histolytica* and that the quantity of Igl varies during phagosome maturation (Okada *et al.* 2005, 2006). The different localization of Igl1 and Igl2 in vacuoles suggests that the functions of the two Igls may differ or that their expression may vary during maturation of phagosomes or depending on certain cellular conditions. However, there may also be differences in the involvement of microtubules and proteases in phagosome maturation and degradation in *E. histolytica* and *E. dispar* (Mitra *et al.* 2005). In *E. histolytica*, different subcellular localization of the two Igl isoforms has yet to be shown.

In conclusion, this is the first study of the differences between Igl1 and Igl2 of *E. dispar*. Igl seems to be a vaccine candidate for amebiasis and may also be a useful antigenic molecule for specific serodiagnosis of amoebiasis (Cheng and Tachibana, 2001; Tachibana *et al.* 2004). Therefore, further studies of Igl are required to clarify its role in the host-parasite relationship.

This work was supported by a Grant-in-Aid for Scientific Research from the Japanese Society for the Promotion of Science, and a grant for Research on Emerging and Re-emerging Infectious Diseases from the Ministry of Health, Labour and Welfare of Japan. X.-J. C. is a recipient of a Postdoctoral Fellowship for Foreign Researchers from the Japanese Society for the Promotion of Science.

REFERENCES

Bruchhaus, I., Jacobs, T., Leippe, M. and Tannich, E. (1996). *Entamoeba histolytica* and *Entamoeba dispar*: differences in numbers and expression of cysteine proteinase genes. *Molecular Microbiology* **22**, 255–263.

Cheng, X.-J., Hughes, M. A., Huston, C. D., Loftus, B., Gilchrist, C. A., Lockhart, L. A., Ghosh, S., Miller-Sims, V., Mann, B. J., Petri, W. A., Jr. and Tachibana, H. (2001). Intermediate subunit of the Gal/GalNAc lectin of *Entamoeba histolytica* is a member of a gene family containing multiple CXXC sequence motifs. *Infection and Immunity* **69**, 5892–5898.

Cheng, X.-J., Kaneda, Y. and Tachibana, H. (1997). A monoclonal antibody against the 150-kDa surface antigen of *Entamoeba histolytica* inhibits adherence and cytotoxicity to mammalian cells. *Medical Science Research* **25**, 159–161.

Cheng, X.-J. and Tachibana, H. (2001). Protection of hamsters from amebic liver abscess formation by immunization with the 150- and 170-kDa surface antigens of *Entamoeba histolytica*. *Parasitology Research* **87**, 126–130.

Cheng, X.-J., Tachibana, H. and Kaneda, Y. (1999). Protection of hamsters from amebic liver abscess formation by a monoclonal antibody to a 150-kDa surface lectin of *Entamoeba histolytica*. *Parasitology Research* **85**, 78–80.

Cheng, X.-J., Tsukamoto, H., Kaneda, Y. and Tachibana, H. (1998). Identification of the 150-kDa surface antigen of *Entamoeba histolytica* as a galactose- and *N*-acetyl-D-galactosamine-inhibitable lectin. *Parasitology Research* **84**, 632–639.

Davis, P. H., Schulze, J. and Stanley, S. L., Jr. (2007). Transcriptomic comparison of two *Entamoeba histolytica* strains with defined virulence phenotypes identifies new virulence factor candidates and key differences in the expression patterns of cysteine proteases, lectin light chains, and calmodulin. *Molecular and Biochemical Parasitology* **151**, 118–128.

Diamond, L. S. and Clark, C. G. (1993). A redescription of *Entamoeba histolytica* Schaudinn, 1903 (Emended Walker, 1911) separating it from *Entamoeba dispar* Brumpt, 1925. *Journal of Eukaryotic Microbiology* **40**, 340–344.

Diamond, L. S., Harlow, D. R. and Cunnick, C. C. (1978). A new medium for the axenic cultivation of *Entamoeba histolytica* and other *Entamoeba*. *Transactions of the Royal Society of Tropical Medicine and Hygiene* **72**, 431–432.

Hernández-Ramírez, V. I., Rios, A., Angel, A., Magos, M. A., Pérez-Castillo, L., Rosales-Encina, J. L., Castillo-Henkel, E. and Talamás-Rohana, P. (2007). Subcellular distribution of the *Entamoeba histolytica* 140 kDa FN-binding molecule during host-parasite interaction. *Parasitology* **134**, 169–177.

Khalifa, S. A., Imai, E., Kobayashi, S., Haghighi, A., Hayakawa, E. and Takeuchi, T. (2006). Growth-promoting effect on iron-sulfur proteins on axenic cultures of *Entamoeba dispar*. *Parasite* **13**, 51–58.

Kobayashi, S., Imai, E., Haghighi, A., Khalifa, S. A., Tachibana, H. and Takeuchi, T. (2005). Axenic cultivation of *Entamoeba dispar* in newly designed yeast extract-iron-gluconic acid-dihydroxyacetone-serum medium. *Journal of Parasitology* **91**, 1–4.

Laemmli, U. K. (1970). Cleavage of structural proteins during the assembly of the head of bacteriophage T4. *Nature, London* **227**, 680–685.

MacFarlane, R. C. and Singh, U. (2006). Identification of differentially expressed genes in virulent and nonvirulent *Entamoeba* species: potential implications for amebic pathogenesis. *Infection and Immunity* **74**, 340–351.

McCoy, J. J. and Mann, B. J. (2005). Proteomic analysis of Gal/GalNAc lectin-associated proteins in *Entamoeba histolytica*. *Experimental Parasitology* **110**, 220–225.

Mitra, B. N., Yasuda, T., Kobayashi, S., Saito-Nakano, Y. and Nozaki, T. (2005). Differences in morphology of phagosomes and kinetics of acidification and degradation in phagosomes between the pathogenic *Entamoeba histolytica* and the non-pathogenic *Entamoeba dispar*. *Cell Motility and the Cytoskeleton* **62**, 84–99.

Okada, M., Huston, C. D., Mann, B. J., Petri, W. A., Jr. Kita, K. and Nozaki, T. (2005). Proteomic analysis of phagocytosis in the enteric protozoan parasite *Entamoeba histolytica*. *Eukaryotic Cell* **4**, 827–831.

Okada, M., Huston, C. D., Oue, M., Mann, B. J., Petri, W. A., Jr. Kita, K. and Nozaki, T. (2006). Kinetics and strain variation of phagosome proteins of *Entamoeba histolytica* by proteomic analysis. *Molecular and Biochemical Parasitology* **145**, 171–183.

Petri, W. A., Jr. Chapman, M. D., Snodgrass, T., Mann, B. J., Broman, J. and Ravdin, J. I. (1989). Subunit structure of the galactose and *N*-acetyl-D-galactosamine-inhibitable adherence lectin of *Entamoeba histolytica*. *Journal of Biological Chemistry* **264**, 3007–3012.

Petri, W. A., Jr. Haque, R. and Mann, B. J. (2002). The bittersweet interface of parasite and host: lectin-carbohydrate interactions during human invasion by the parasite *Entamoeba histolytica*. *Annual Review of Microbiology* **56**, 39–64.

Pillai, D. R., Britten, D., Ackers, J. P., Ravdin, J. I. and Kain, K. C. (1997). A gene homologous to hgl2 of *Entamoeba histolytica* is present and expressed in *Entamoeba dispar*. *Molecular and Biochemical Parasitology* **87**, 101–105.

Pillai, D. R., Kobayashi, S. and Kain, K. C. (2001). *Entamoeba dispar*: molecular characterization of the galactose/*N*-acetyl-D-galactosamine lectin. *Experimental Parasitology* **99**, 226–234.

Seigneur, M., Mounier, J., Prevost, M. C. and Guillen, N. (2005). A lysine- and glutamic acid-rich protein, KERP1, from *Entamoeba histolytica* binds to human enterocytes. *Cellular Microbiology* **7**, 569–579.

Shah, P. H., MacFarlane, R. C., Bhattacharya, D., Matese, J. C., Demeter, J., Stroup, S. E. and Singh, U. (2005). Comparative genomic hybridizations of *Entamoeba* strains reveal unique genetic fingerprints that correlate with virulence. *Eukaryotic Cell* **4**, 504–515.

Tachibana, H., Cheng, X.-J., Masuda, G., Horiki, N. and Takeuchi, T. (2004). Evaluation of recombinant fragments of *Entamoeba histolytica* Gal/GalNAc lectin intermediate subunit for serodiagnosis of amebiasis. *Journal of Clinical Microbiology* **42**, 1069–1074.

Tachibana, H., Ihara, S., Kobayashi, S., Kaneda, Y., Takeuchi, T. and Watanabe, Y. (1991). Differences in genomic DNA sequences between pathogenic and nonpathogenic isolates of *Entamoeba histolytica* identified by polymerase chain reaction. *Journal of Clinical Microbiology* **29**, 2234–2239.

Tachibana, H., Kobayashi, S., Cheng, X.-J. and Hiwatashi, E. (1997). Differentiation of *Entamoeba histolytica* from *E. dispar* facilitated by monoclonal antibodies against a 150-kDa surface antigen. *Parasitology Research* **83**, 435–439.

Talamás-Rohana, P., Rosales-Encina, J. L., Gutierrez, M. C. and Hernández, V. I. (1992). Identification and partial purification of an *Entamoeba histolytica* membrane protein that binds fibronectin. *Archives of Medical Research* **23**, 119–123.

Walsh, J. A. (1986). Problems in recognition and diagnosis of amebiasis: estimation of the global magnitude of morbidity and mortality. *Reviews of Infectious Diseases* **8**, 228–238.

Weber, C., Guigon, G., Bouchier, C., Frangeul, L., Moreira, S., Sismeiro, O., Gouyette, C., Mirelman, D., Coppee, J. Y. and Guillen, N. (2006). Stress by heat shock induces massive down regulation of genes and allows differential allelic expression of the Gal/GalNAc lectin in *Entamoeba histolytica*. *Eukaryotic Cell* **5**, 871–875.

Willhoeft, U., Hamann, L. and Tannich, E. (1999). A DNA sequence corresponding to the gene encoding cysteine proteinase 5 in *Entamoeba histolytica* is present and positionally conserved but highly degenerated in *Entamoeba dispar*. *Infection and Immunity* **67**, 5925–5929.

Serum Indicators for the Diagnosis of Pneumocystis Pneumonia*

Sadatomo Tasaka, MD, FCCP; Naoki Hasegawa, MD; Seiki Kobayashi, MD; Wakako Yamada, MD; Tomoyasu Nishimura, MD; Tsutomu Takeuchi, MD; and Akitoshi Ishizaka, MD

Background: **The diagnosis of pneumocystis pneumonia (PCP) is difficult because it requires microscopic examination to identify pneumocystis from induced sputum or BAL fluid.**
Study objective: **To evaluate the usefulness of four serum markers—lactate dehydrogenase (LDH), (1→3) β-D-glucan (β-D-glucan), KL-6, and C-reactive protein (CRP)—in the diagnosis of PCP.**
Design: **Case-control retrospective study.**
Patients and measurements: **We reviewed the medical records of 295 consecutive patients who underwent BAL for the diagnosis of PCP. Differential cell counts in BAL fluid and serum levels of LDH, β-D-glucan, KL-6, and CRP were examined. Oxygenation index was determined using arterial oxygen tension and inspiratory oxygen concentration.**
Results: **Based on the microscopic examination of BAL fluid, 57 patients were PCP positive and 238 patients were PCP negative. There were no significant differences in cell count or differentials in BAL fluid between the positive and negative cases. Serum levels of LDH, β-D-glucan, and KL-6 were significantly higher in PCP-positive patients ($p < 0.01$). Receiver operating characteristic curves suggest that β-D-glucan was the most reliable indicator. The cut-off level of β-D-glucan was estimated to be 31.1 pg/mL, with which the positive and negative predictive values were 0.610 and 0.980, respectively. In PCP-positive patients, the oxygenation index was decreased and correlated with LDH. Both LDH and β-D-glucan levels were correlated with the proportion of neutrophils in BAL fluid.**
Conclusions: **Serum β-D-glucan is a reliable marker for the diagnosis of PCP. Since BAL procedure is invasive, measuring β-D-glucan should be considered as a primary modality for a diagnosis of PCP, especially for patients with severe respiratory failure.** ***(CHEST 2007; 131:1173–1180)***

Key words: BAL; (1→3)-β-D-glucan; KL-6; lactate dehydrogenase; pneumocystis pneumonia

Abbreviations: β-D-glucan = (1→3) β-D-glucan; CRP = C-reactive protein; F_{IO_2} = fraction of inspired oxygen; GMS = Grocott-Gomori methenamine stain; LDH = lactate dehydrogenase; NPV = negative predictive value; PCP = pneumocystis pneumonia; PCR = polymerase chain reaction; PPV = positive predictive value; ROC = receiver operating characteristic

Pneumocystis pneumonia (PCP) remains one of the most frequent opportunistic infections in immunocompromised patients, including those with HIV infection.[1] PCP may be difficult to diagnose owing to nonspecific symptoms and signs, concurrent use of prophylactic drugs, and simultaneous infection with various organisms. Since pneumocystis cannot be cultured, the diagnosis of PCP requires microscopic examination in order to identify *Pneumocystis jirovecii* from a clinically relevant source such as specimens of induced sputum, BAL fluid, or lung tissue.

Sputum induction with hypertonic saline solution should be the initial procedure to diagnose PCP, especially in patients with AIDS. The induced sputum has a diagnostic yield of 50 to 90%. However, the diagnostic yield is unsatisfactory, particularly in the case of a non-AIDS immunocompromised patient. If the initial specimen of induced sputum is negative, then bronchoscopy with BAL, which is invasive particularly for those with respiratory failure, should be performed.[2]

Serum testing for the diagnosis of PCP has not yet been established. Although an elevated serum lactate

Reprinted from CHEST
Vol. 131, p. 1173-1180, April 2007 Issue

dehydrogenase (LDH) level has been noted in patients with PCP, it is likely to be a reflection of the underlying lung inflammation and injury rather than a specific marker for the disease.[3]

(1→3) β-D-glucan (β-D-glucan), which is known to compose a portion of the cell wall of most fungi, has been used as a serologic marker for the diagnosis of organic mycosis, such as candidiasis and aspergillosis.[4] There have been several reports[5,6] describing the usefulness of β-D-glucan for the diagnosis of PCP based on data from small numbers of patients. KL-6 antigen, a high-molecular-weight mucin-like glycoprotein, is strongly expressed on type 2 alveolar pneumocytes and bronchiolar epithelial cells, and the serum KL-6 level is a sensitive indicator of various types of interstitial pneumonitis.[7] KL-6 levels in both plasma and epithelial lining fluid appear to be elevated in patients with acute lung injury.[8] There have been two reports[9,10] describing increased serum KL-6 levels in patients complicated with PCP. The usefulness of these newly identified serum markers in the diagnosis of PCP remains to be evaluated in a larger cohort of patients.

The primary goal of the present study was to evaluate the sensitivity and specificity of the serum markers LDH, β-D-glucan, KL-6, and C-reactive protein (CRP) in the diagnosis of PCP. We also examined whether the serum markers reflect oxygenation impairment and activity of lung inflammation during PCP.

Materials and Methods

Patient Selection

We retrospectively evaluated data from 295 consecutive patients who underwent BAL for the diagnosis of PCP at Keio University Hospital (Tokyo, Japan) during the period from April 1998 until October 2005.

Data Collection

We reviewed the medical records of all the patients evaluated for demographic, BAL, and serum data. The following data were collected: age, sex, and underlying disease. The BAL data included the recovery of the fluid, which is the volume ratio of the saline solution recovered to the saline solution instilled, the cell count and differentials, plus lymphocyte surface markers. In sera, the levels of LDH, β-D-glucan, KL-6, and CRP were examined. β-D-glucan was measured with a kinetic turbidimetric assay using β-glucan test WAKO (Wako Pure Chemical Industries; Tokyo, Japan). KL-6 was measured by electrochemiluminescence immunoassay using KL-6 antibody, which recognizes a sialylated sugar chain on the KL-6 molecule. The oxygenation index was determined from the arterial oxygen tension and fraction of inspired oxygen (F_{IO_2}) values. Serologic and blood gas data were subjected to analysis only when obtained within 24 h prior to BAL.

BAL Procedure

The diagnosis of PCP was established by the identification of organisms in BAL fluid. Informed consent to conduct BAL was obtained from either the patient or surrogate. In most cases, BAL was targeted toward affected lung segments as noted on chest CT and performed with 50 mL of 0.9% saline solution per lavage. Usually, three lavages were performed, and the lavage fluid was immediately placed on ice.

BAL Fluid Processing for Analysis

The BAL fluid was pooled, filtered through sterile gauze to remove mucous strands, and centrifuged at 200g for 5 min at 4°C. The cell pellets were used for the differential counts on Wright-Giemsa-stained preparations. For the detection of *P jirovecii*, a 10-mL aliquot of BAL fluid was centrifuged at 1,875g for 10 min, and a smear was microscopically examined for the presence of *P jirovecii* with Grocott-Gomori methenamine stain (GMS) and Calcofluor white stain (Fungifluor; Polysciences; Warington, PA), following the recommendations of the manufacturer.[11]

Statistical Methods

Data are presented as the median score with interquartile range in parentheses. Differences in variables between the PCP-positive and PCP-negative patients were compared by the nonparametric Mann-Whitney *U* test since the data were not normally distributed. Box-and-whisker plots represent the 10th, 25th, 50th, 75th, and 95th percentile of values. To evaluate the sensitivity and specificity of each serum marker, receiver operating characteristic (ROC) curves were constructed for each marker. The areas under the ROC curves were compared in a nonparametric approach.[12] The relationships between variables were analyzed by the Spearman rank-order correlation test. Statistical significance was defined as $p < 0.05$.

Results

During the study period, PCP was diagnosed in 57 patients based on microscopic findings in BAL specimens. A total of 238 patients were PCP negative, 16 of whom were empirically treated with trimethoprim/sulfamethoxazole or pentamidine due to persistent suspicion about PCP or failure of the preceding treatment. Data from these 16 patients were excluded from the analysis because it was

*From the Departments of Medicine (Drs. Tasaka, Hasegawa, Yamada, Nishimura, and Ishizaka) and Tropical Medicine and Parasitology (Drs. Kobayashi and Takeuchi), Keio University School of Medicine, Tokyo, Japan.
None of the authors have any conflicts of interest to disclose.
Manuscript received June 10, 2006; revision accepted November 16, 2006.

Correspondence to: Sadatomo Tasaka, MD, FCCP, Division of Pulmonary Medicine, Keio University School of Medicine, 35 Shinanomachi, Shinjuku-ku, Tokyo 160-8582, Japan; e-mail: tasaka@cpnet.med.keio.ac.jp
DOI: 10.1378/chest.06-1467

Table 1—*Patient Characteristics

Characteristics	PCP Positive (n = 57)	PCP Negative (n = 222)	p Value†
Age, yr	42.5 (34.0–58.0)	58.0 (47.0–68.0)	< 0.0001
Male/female gender, No	36/21	117/105	
Underlying disease, No			
Hematologic malignancy	14	88	
HIV	13	3	
Collagen vascular disease	11	40	
Interstitial lung disease	5	32	
Organ transplantation	5	11	
Lung cancer	4	19	
Other	5	29	
PaO_2/FIO_2‡	241.5 (143.2–323.4)	311.0 (207.6–376.4)	0.009

*Data are presented as median (interquartile range) unless otherwise indicated.
†Mann-Whitney *U* test.
‡Oxygenation index.

thought that they may have had PCP. All of the PCP-positive patients were treated initially with trimethoprim/sulfamethoxazole, and 13 of them subsequently received pentamidine due to failure or adverse effects of the trimethoprim/sulfamethoxazole treatment.

The background characteristics and oxygenation indices of the patients analyzed are shown in Table 1. The patients with PCP were significantly younger than those without PCP ($p < 0.0001$). The common underlying diseases of the patients with PCP included hematologic malignancy, HIV infection, and collagen vascular disease. The oxygenation index in the patients with PCP was significantly lower than in those without PCP ($p = 0.009$).

The underlying diseases of the 16 patients excluded from analyses include hematologic malignancies (n = 6), collagen vascular diseases (n = 4), lung cancer (n = 3), other malignancies (n = 2), and Crohn disease (n = 1). Most of these 16 patients were immunocompromised due to preceding antineoplastic or corticosteroid therapy. No evidence of PCP was observed in any of these patients. The most probable diagnoses of those 16 patients include alveolar hemorrhage (n = 3), radiation pneumonitis (n = 2), drug-induced pneumonitis (n = 2), pneumonia due to *Pseudomonas aeruginosa* (n = 2), cytomegalovirus pneumonia (n = 2), and invasive pulmonary aspergillosis (n = 1). The rest of the patients were treated as having pneumonia due to an unidentified pathogen. Even if the 16 patients were included in the analysis, the results were not changed (data not shown).

The recovery rate, cell counts, and differentials of BAL fluid are summarized in Table 2. Neither the recovery rate nor total cell count of BAL fluid were different between the PCP-positive and PCP-negative patients. There were no differences in the proportions of macrophages, lymphocytes, neutrophils, and eosinophils in BAL fluid between the

Table 2—*BAL Cell Counts and Differentials

Parameters	PCP Positive (n = 57)	PCP Negative (n = 222)	p Value†
BAL			
Fluid recovery, %	45.0 (32.3–54.5)	40.0 (30.0–50.0)	0.13
Cell concentration, $\times 10^5$/mL	5.9 (3.0–11.9)	8.7 (4.4–15.0)	0.054
Macrophages, %	36.5 (18.3–57.0)	39.8 (22.6–60.5)	0.52
Lymphocytes, %	28.5 (13.5–53.0)	32.1 (13.2–56.9)	0.73
Neutrophils, %	9.0 (3.0–35.1)	6.7 (1.8–26.7)	0.41
Eosinophils, %	0.4 (0.0–1.8)	0.5 (0.0–2.1)	0.33
$CD4^+/CD8^+$ ratio	0.53 (0.33–1.45)	1.00 (0.54–1.80)	0.039
Peripheral blood			
WBC count, $\times 10^3/\mu L$	6.7 (3.6–9.3)	6.6 (4.2–9.9)	0.64
Neutrophils, %	88.0 (76.9–94.0)	79.0 (64.9–89.4)	0.003
Lymphocytes, %	6.0 (3.8–11.3)	10.0 (4.0–18.9)	0.011

*Data are presented as median (interquartile range).
†Mann-Whitney *U* test.

PCP-positive and PCP-negative patients. The $CD4^+/CD8^+$ ratio of the lymphocytes in the BAL fluid was significantly decreased in patients with PCP compared to those without PCP ($p = 0.039$). Peripheral leukocyte counts are also shown in Table 2. In peripheral blood, WBC counts did not differ between the PCP-positive and PCP-negative patients. However, in patients with PCP, the proportion of neutrophils in circulating WBC was greater than in those without PCP ($p = 0.003$). The proportion of lymphocytes in peripheral blood was decreased in the PCP-positive patients compared to that in the PCP-negative patients ($p = 0.011$; Table 2).

We measured serum markers (LDH, β-D-glucan, KL-6, and CRP) and compared the levels between the PCP-positive and PCP-negative patients. The serum LDH levels were significantly higher in the PCP-positive patients than in the PCP-negative patients, despite the underlying disease ($p < 0.0001$; Fig 1, *top left, A*). Serum β-D-glucan levels were also significantly increased in the PCP-positive patients ($p < 0.0001$; Fig 1, *top right, B*). Figure 1, *bottom left, C* shows that the serum KL-6 levels were significantly increased in the PCP-positive patients compared to the PCP-negative patients ($p = 0.004$). Among the PCP-negative patients, there were 19 patients with serum KL-6 levels > 1,000 U/mL, and

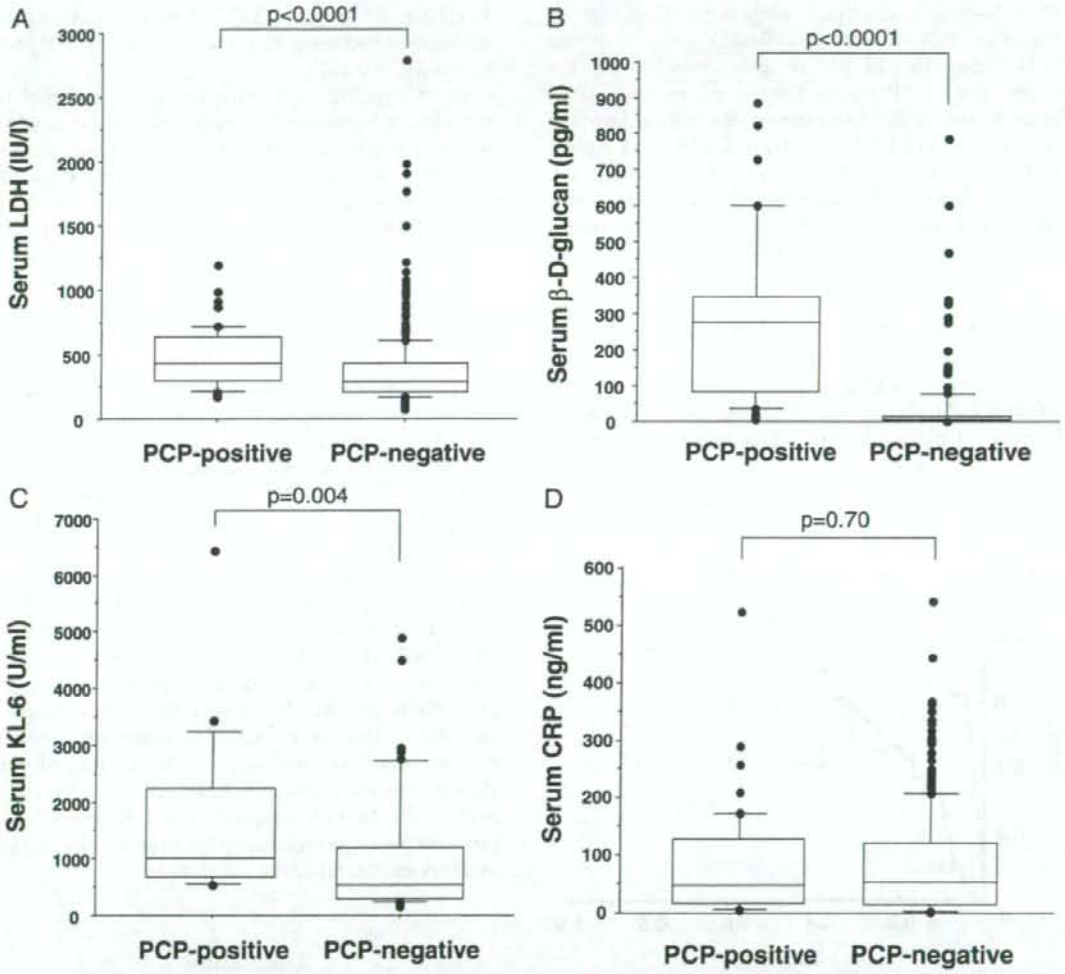

FIGURE 1. Serum markers of LDH (*top left, A*), β-D-glucan (*top right, B*), KL-6 (*bottom left, C*), and CRP (*bottom right, D*) in patients with PCP and those without PCP. The box-and-whisker plots show the 25th and 75th percentiles, the median (horizontal line within the box), and the 10th and 90th percentiles (whiskers). Serum levels of LDH, β-D-glucan, and KL-6 were significantly higher in PCP patients ($p < 0.01$).